

Leaf xylem embolism, detected acoustically and by cryo-SEM, corresponds to decreases in leaf hydraulic conductance in four evergreen species

DANIEL M. JOHNSON¹, FREDERICK C. MEINZER¹, DAVID R. WOODRUFF¹ & KATHERINE A. MCCULLOH²

¹USDA Forest Service, Pacific Northwest Research Station, OR 97331, USA and ²Department of Wood Science and Engineering, Oregon State University, Corvallis, OR 97331, USA

ABSTRACT

Hydraulic conductance of leaves (K_{leaf}) typically decreases with increasing water stress. However, the extent to which the decrease in K_{leaf} is due to xylem cavitation, conduit deformation or changes in the extra-xylary pathway is unclear. We measured K_{leaf} concurrently with ultrasonic acoustic emission (UAE) in dehydrating leaves of two vessel-bearing and two tracheid-bearing species to determine whether declining K_{leaf} was associated with an accumulation of cavitation events. In addition, images of leaf internal structure were captured using cryo-scanning electron microscopy, which allowed detection of empty versus full and also deformed conduits. Overall, K_{leaf} decreased as leaf water potentials (Ψ_L) became more negative. Values of K_{leaf} corresponding to bulk leaf turgor loss points ranged from 13 to 45% of their maximum. Additionally, Ψ_L corresponding to a 50% loss in conductivity and 50% accumulated UAE ranged from -1.5 to -2.4 MPa and from -1.1 to -2.8 MPa, respectively, across species. Decreases in K_{leaf} were closely associated with accumulated UAE and the percentage of empty conduits. The mean amplitude of UAEs was tightly correlated with mean conduit diameter ($R^2 = 0.94$, $P = 0.018$). These results suggest that water stress-induced decreases in K_{leaf} in these species are directly related to xylem embolism.

Key-words: cavitation; drought stress; transpiration; water potential.

INTRODUCTION

When the transport of water to leaves is insufficient to resupply water during periods of rapid transpiration or drought, leaves tend to dehydrate. Hydraulic conductance in leaves (K_{leaf}) decreases as leaves desiccate, resulting in reduced water transport capacity and eventually stomatal closure and, thus, negligible photosynthesis (see Sack & Holbrook 2006 and references therein). However, the extent to which the observed fluctuations in K_{leaf} are related to reversible xylem cavitation, reversible partial conduit

collapse or changes in the extra-xylary portion of the hydraulic pathway is uncertain (Sack & Holbrook 2006). Moreover, the relative importance of mechanisms contributing to variation in K_{leaf} may differ among species.

Recent work has provided evidence that water stress-induced reductions in K_{leaf} resulted from leaf xylem cavitation (e.g. Bucci *et al.* 2003; Nardini, Salleo & Raimondo 2003; Woodruff *et al.* 2007). However, decreases in K_{leaf} in dehydrating pine needles appeared to be due to xylem element collapse, which occurred at less negative water potentials than cavitation (Cochard *et al.* 2004). Models have predicted that embolism should occur at less negative water potentials than implosion in stems and roots (Hacke *et al.* 2001; Hacke, Sperry & Pittermann 2004), although this may not be true for leaves. It is possible that walls of xylem conduits in leaves are less resistant to collapse, as compared to walls of secondary xylem conduits in stems and roots. Xylem collapse in leaves could be related to reduced mechanical support inside leaves as compared to wood. In addition, deformed conduits may be easier to refill under negative pressure than embolized conduits (Tyree & Yang 1992; Cochard *et al.* 2004).

Changes to extra-xylary pathways of water transport inside the leaf could also have a strong influence on K_{leaf} because the extra-xylary portion of the pathway may make up as much as 70% of the overall hydraulic resistance of leaves (Sack, Streeter & Holbrook 2004; Nardini & Salleo 2005; Brodribb, Field & Jordan 2007; Mott 2007). Therefore, changes in cell membrane permeability (e.g. via aquaporins) could have large impacts on K_{leaf} (Cochard *et al.* 2007; Kaldenhoff *et al.* 2008; Voicu, Zwiazek & Tyree 2008). Another example of extra-xylary impacts on K_{leaf} is the collapse of accessory transfusion tracheids in *Podocarpus grayi*, which coincided with depressions of K_{leaf} during dehydration (Brodribb & Holbrook 2005).

Ultrasonic acoustic emission (UAE) has been used for decades to detect cavitation events in tree stems (Millburn & Johnson 1966; Tyree & Dixon 1983; Nardini & Salleo 2000) and, more recently, in leaves (Kikuta *et al.* 1997; Nardini, Tyree & Salleo 2001; Salleo *et al.* 2001). During cavitation events, waves of energy likely result from sudden relaxation of tension inside the conduit lumen as air replaces water (Tyree & Sperry 1989). In wood, cavitation

Correspondence: D. M. Johnson. Fax: +1 541 750 7250; e-mail: danieljohnson@fs.fed.us

events can occur in both conductive (tracheids and vessels) and non-conductive elements (ray tracheids and fibres). Furthermore, a single acoustic emission can cause a decline in the total hydraulic conductance by varying amounts depending on the diameter of the conduit. This can result in a relationship between hydraulic conductance and accumulated acoustic emissions that is not proportional (Rosner *et al.* 2006). However, because the vascular bundles of leaves are composed nearly entirely of xylem and phloem, we would expect close correspondence between accumulated acoustic emissions and K_{leaf} . Additionally, it has been proposed that the frequency range and/or amplitude of UAEs may be related to the dimensions of the cavitating conduits (Ritman & Milburn 1988, 1991; Rosner *et al.* 2006).

In the present study, we measured hydraulic conductance and UAEs in drying leaves of four evergreen species: two conifers and two angiosperms. Our goals were to assess the coordination between accumulated emissions and depressions in K_{leaf} and to assess the extent to which water stress-induced loss of K_{leaf} was associated with xylem cavitation. Additionally, cryo-scanning electron microscopy (cryo-SEM) was performed on leaf samples flash-frozen at different water potentials as an independent measure of xylem embolism and to detect xylem deformation or changes in the distribution of water within leaves as they dried.

MATERIALS AND METHODS

Plant material

Four evergreen woody species were chosen as representative of tracheid-bearing and vessel-bearing species as well as based on local occurrence. Shoots of three to five individuals of *Pinus ponderosa* C. Lawson, *Pinus nigra* Arnold, *Castanopsis chrysophylla* (Dougl.) A. DC., and *Pieris japonica* (Thunb.) D. Don ex G. Don were collected between October 2007 and March 2008, sealed in plastic bags and returned to the lab. All samples were collected from branches in full sunlight from individuals >2 m in height. All leaves used in this study were from the previous year and were fully expanded. Samples were collected from Oregon State University Campus, McDonald-Dunn University Forest and Dan Farmer Tree Farm, all located near Corvallis, OR, USA.

K_{leaf} and vulnerability

Leaf hydraulic conductance was determined using a timed rehydration method described in Brodribb & Holbrook (2003), which involved the use of the following equation based on an analogy between rehydrating a leaf and recharging a capacitor:

$$K_{\text{leaf}} = C \ln(\Psi_o / \Psi_t) / t$$

where C = capacitance, Ψ_o = leaf water potential before partial rehydration, Ψ_t = leaf water potential after partial rehydration and t = duration of rehydration. Branches approximately 30–50 cm long were collected from trees

early in the morning before significant transpirational water loss and were transported back to the lab, recut under water and allowed to rehydrate for at least 4 h. Shoots were dried on the bench top for varying lengths of time, placed in a plastic bag and sealed and then kept in the dark for at least 1 h to equilibrate. Measurements of leaf water potential were conducted over the next 3 d (shoots kept in the dark at 4 °C, unless measured on the same day as they were dehydrated) on excised leaves/fascicles for initial values (Ψ_o), and for final values after a period of rehydration of t seconds (Ψ_t), which was between 30 and 120 s. Distilled water was used for rehydration of K_{leaf} samples and water temperature was maintained between 21 and 23 °C. The photosynthetic photon flux density at the foliage was maintained at approximately 1000 $\mu\text{mol m}^{-2} \text{s}^{-1}$ during K_{leaf} measurements.

Values of C were estimated from pressure–volume curves (Scholander *et al.* 1965; Tyree & Hammel 1972) using the methods described by Brodribb & Holbrook (2003) for three to six leaves of each species. Briefly, the Ψ_L corresponding to turgor loss was estimated as the inflection point (the transition from the initial curvilinear, steeper portion of the curve to the more linear, less steep portion) of the graph of Ψ_L versus relative water content (RWC). The slope of the curve before and after turgor loss provided C in terms of RWC (C_{rwc}) for pre-turgor loss and post-turgor loss, respectively.

Pressure–volume curves were conducted on individual leaves for the broadleaf species and on fascicles of three needles for the two *Pinus* species. Branch samples of approximately 30–50 cm were excised early in the morning and recut under water in the lab. Branches were allowed to rehydrate for at least 4 h before pressure–volume analyses were performed. Pressure–volume curves were created by plotting the inverse of Ψ_L against RWC, and alternate determinations of fresh mass and Ψ_L were repeated during slow dehydration of the twig on the laboratory bench until values of Ψ_L exceeded the measuring range of the pressure chamber (–4.0 MPa). Leaf water potential was measured using a pressure chamber (PMS Instrument Company, Corvallis, OR, USA). For normalizing C on a leaf area basis, leaf areas for the broadleaf species were obtained with a scanner and ImageJ version 1.27 image analysis software (Abramoff, Magelhaes & Ram 2004; National Institute of Mental Health, Bethesda, MD, USA) and needle areas for the *Pinus* species were determined by multiplying mean needle lengths and circumferences (n = six needles per species).

UAE

Shoots were allowed to equilibrate overnight in plastic bags, and six to eight leaves were removed. Two leaves were used for acoustic emission measurements, and three to four leaves were used for water potential measurements. Two sensors (R15 α , Physical Acoustics Corporation, Princeton Junction, NJ, USA) were connected to a UAE-specific data-logger (Pocket AE, Physical Acoustics Corporation) and emissions were amplified by 26 dB. Sensors were placed on

the abaxial surface of each leaf midvein, 2–5 cm from the base of the petiole or fascicle sheath (on the proximal end of the leaf), and leaves were allowed to dry on the bench top for 6–24 h. A small amount of silicone-based grease was placed at the leaf-transducer interface and was also applied to the same area of leaves used for water potential measurements (to minimize variation in treatment conditions). We detected little variation in adaxial versus abaxial UAE, in contrast to earlier work by Kikuta *et al.* (1997). The entire UAE measurement apparatus was acoustically isolated by enclosing it in insulation wrap and 3 cm foam packing material. Leaves used for UAE and those used for water potential measurements were kept in the dark, inside the acoustic isolation material, for the duration of the measurements (except when water potential measurements were performed). Measurement sensitivity was set to 29 dB, below which the instrument detected acoustic signals that were not from leaves [e.g. Radio Frequency Interference (RFI) from fluorescent lights – communication from Physical Acoustics Corp.]. Water potentials of leaves adjacent to the leaves being measured for UAE were measured every 30–60 min while acoustic emission measurements were being made. Experiments were conducted before the study to ensure that, during dehydration, water potentials of UAE leaves were similar to those used for water potential measurements. Mean water potentials for leaves with UAE sensors attached were typically within 3–7% of mean water potential values for leaves without sensors (using two to six leaves for each treatment).

Additionally, to test for introduction of embolism due to removing leaves from stems for UAE measurements, petioles were excised from both *Pieris* and *Castanopsis* leaves, including the proximal third of the midvein (the same approximate location used for both cryo-SEM and UAE) under water, attached to a pressurized air source and pressure was applied to the section (under water) to see if there were air bubbles. Then sections were shortened by approximately 0.5 cm and pressure was applied again. At no point were there bubbles coming from the end of the section, indicating that the vessels were shorter than the section used. This process was repeated until we could not discriminate between air bubbles originating from the coupling of the petiole/midvein to the tubing (approximately 1 cm petiole/midvein left inside tubing).

Cryo-SEM

Shoots were dried on the bench top for varying lengths of time, sealed in a plastic bag and then kept at 4 °C for 1 h to equilibrate. One leaf/fascicle was removed, the shoot was returned to the plastic bag, and Ψ_L was determined. Leaves were selected for cryo-SEM based on Ψ_L that corresponded to different points on Ψ_L versus K_{leaf} and UAE curves. Then one leaf was removed from the shoot; if a broadleaf, the midvein was removed (see next paragraph); and a portion of the midvein/needle was inserted into a fracture rivet (Electron Microscopy Sciences, Hatfield, PA, USA) containing Tissue-Tek Embedding Compound (Sakura Finetek

USA, Torrance, CA, USA). Portions of needles/midveins used for cryo-SEM corresponded to the same approximate location as UAE sensors were placed (approximately 3 cm from the petiole or fascicle sheath).

To minimize the potential for introducing embolism due to severing veins, angiosperm leaves were flash-frozen in liquid nitrogen (LN_2). Subsequently, midribs were excised with scissors that were also cold, and then midveins were dropped back into LN_2 . Midveins were then placed into fracture rivets (room temperature) containing Tissue-Tek and then immediately dropped back into LN_2 (approximately 2 s was required to transfer tissue into rivets and then return it to LN_2). Pine needles were inserted into Tissue-Tek/rivet, and the rivet/needle was dropped into a vial containing LN_2 . The needle was then trimmed, while frozen, around the fracture rivet to leave approximately 0.5 cm of protruding tissue, then immediately placed back into LN_2 . Vials containing samples were then placed into a cryo-shipper (CX500; Taylor-Wharton Cryogenics, Theodore, AL, USA) that had been pre-charged with LN_2 . Samples were shipped to the microscopy facility at University of British Columbia, where they were fractured and imaged. Midveins/needles embedded in fracture rivets were mounted in a cryo-prep apparatus (K1270; Emitech USA, Houston, TX, USA) and were fractured by touching them with a metal prong. They were then sublimed for approximately 10 min and imaged in the cryo-SEM unit (S4700 FESEM; Hitachi High-Technologies Corp., Berkshire, UK).

Seventeen images, each corresponding to a different sample, were quantitatively analysed using ImageJ. The percentage of conduits that were full/empty was determined and all the diameters of all empty conduits were measured. The reported values of mean conduit diameter were determined from images of leaf tissue containing empty conduits.

Statistics/data analysis

For each species, K_{leaf} and UAE data were grouped (binned) over water potential ranges of approximately 0.3 MPa (i.e. –0.61 to –0.90 MPa, –0.91 to –1.20 MPa, etc.) with the exception of the first bin for each species, which corresponded to 0–0.6 MPa. Each bin contained 2–10 leaves, and a total of 42–55 leaves were used for K_{leaf} and 42–65 time points for UAE measurements in each species. However, curves were fitted through non-binned data, which reduced the correlation coefficient but reflected the truer fit of curves through the data. Least squares regression was performed using GraphPad Prism 5.0 (Graphpad Software, San Diego, CA, USA) and sigmoid models were fit through the data. Akaike's Information Criterion was used to decide whether to fit linear or sigmoid models through the data.

RESULTS

Overall, K_{leaf} and cumulative UAEs followed similar trends as Ψ_L declined (Figs 1, 2). Differences between Ψ_L at 50% loss of K_{leaf} and 50% cumulative UAE (Table 1) were small

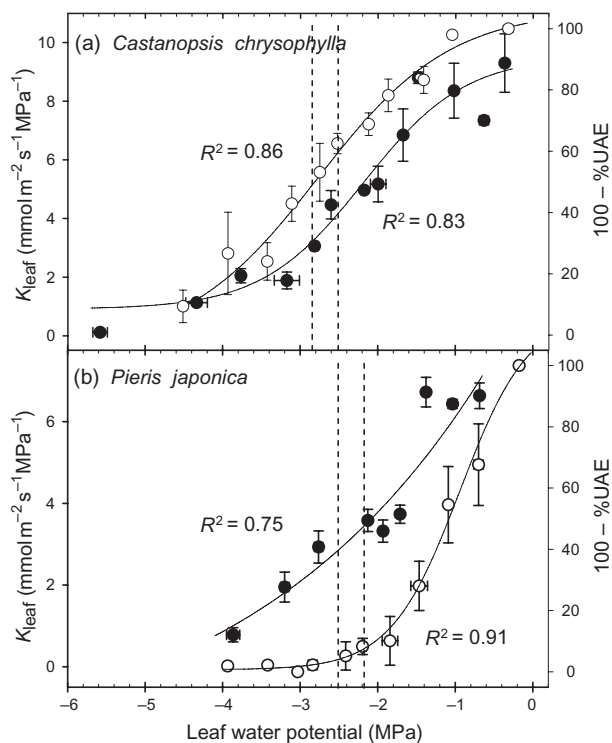


Figure 1. Leaf hydraulic conductance (K_{leaf} , closed circles) and accumulated ultrasonic acoustic emission (UAE, open circles; expressed as 100 – the percentage of total accumulated emissions) at different leaf water potentials for the evergreen broadleaf species (a) *Castanopsis chrysophylla* and (b) *Pieris japonica*. Dashed lines represent mean turgor loss point ± 1 standard error and vertical error bars represent standard error.

in the *Pinus* species (0.13 and 0.29 MPa for *P. nigra* and *P. ponderosa*, respectively), but greater in the two broadleaf species (0.42 and 1.04 MPa in *Castanopsis* and *Pieris*, respectively). At the bulk leaf turgor loss point, K_{leaf} had fallen to approximately 39 and 45% of its maximum value in *Castanopsis* and *Pieris*, respectively, and only 13 and 21% of its maximum in *P. nigra* and *P. ponderosa* (Figs 1, 2, Table 2). Additionally, turgor loss in *Pieris*, *P. nigra* and *P. ponderosa* corresponded to 95, 88 and 84% cumulative UAE, respectively, but only 46% cumulative UAE in *Castanopsis*.

Mean amplitude of UAE was greater in *P. ponderosa* (38.8 dB) than in the other species in the study, and *Castanopsis* had the lowest overall amplitude (32.8 dB, Fig. 3). In

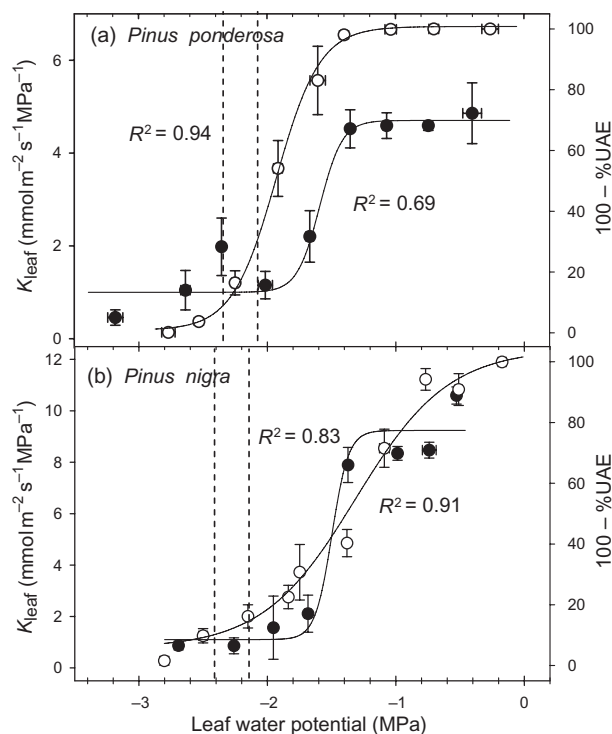


Figure 2. Leaf hydraulic conductance (K_{leaf} , closed circles) and accumulated ultrasonic acoustic emission (UAE, open circles; expressed as 100 – the percentage of total accumulated emissions) at different leaf water potentials for the evergreen needle-leaved species (a) *Pinus ponderosa* and (b) *Pinus nigra*. Dashed lines represent mean turgor loss point ± 1 standard error and vertical error bars represent standard error.

addition, mean amplitude of UAE was strongly correlated to mean conduit size ($R^2 = 0.94$, $P = 0.018$, Figs 3, 4), and the lower detection limit of UAE corresponded to a conduit size of approximately $4.5 \mu\text{m}$.

At full hydration (Ψ_L approximately -0.1 MPa), no xylem conduits were empty in any of the four species, but, as leaves desiccated, an increasing fraction of conduits appeared to be embolized in cryo-SEM images (Figs 5, 6). In addition, the majority of transfusion tissue surrounding the vascular bundles of *P. ponderosa* was empty at -1.4 MPa (Fig. 5c), a water potential that corresponded to only 4% of accumulated UAE and approximately 92% of maximum K_{leaf} . At a given Ψ_L , the percentage of conduits that remained water-filled in cryo-SEM images was strongly

Table 1. Leaf water potential values (Ψ_L), from best-fit regressions, corresponding to 10 and 50% of total accumulated emissions and 10 and 50% loss in K_{leaf} . Numbers in parentheses represent 95% confidence intervals

| Species | Ψ_L at 10% UAE | Ψ_L at PLC10 | Ψ_L at 50% UAE | Ψ_L at PLC50 |
|---------------------------------|---------------------|---------------------|---------------------|---------------------|
| <i>Castanopsis chrysophylla</i> | -1.29 (-0.98/-1.56) | -1.11 (-0.40/-1.44) | -2.82 (-2.68/-2.97) | -2.40 (-2.20/-2.60) |
| <i>Pieris japonica</i> | -0.43 (-0.19/-0.58) | -0.87 (-0.50/-1.12) | -1.08 (-0.94/-1.22) | -2.12 (-1.90/-2.31) |
| <i>Pinus nigra</i> | -0.67 (-0.50/-0.85) | -1.37 (-1.25/-1.46) | -1.39 (-1.28/-1.52) | -1.52 (-1.47/-1.57) |
| <i>Pinus ponderosa</i> | -1.58 (-1.49/-1.65) | -1.43 (-1.08/-1.55) | -1.94 (-1.90/-1.97) | -1.65 (-1.54/-1.75) |

PLC, percent loss of conductance.

| Species | TLP (MPa) | % $K_{\text{leaf-max}}$ at TLP | Pre-TLP C (mol m ⁻² MPa ⁻¹) | Post-TLP C (mol m ⁻² MPa ⁻¹) |
|------------------------|--------------|--------------------------------|---|--|
| <i>Castanopsis</i> | -2.68 (0.17) | 39 | 0.51 (0.02) | 0.70 (0.03) |
| <i>Pieris</i> | -2.37 (0.18) | 45 | 0.74 (0.07) | 1.33 (0.18) |
| <i>Pinus nigra</i> | -2.28 (0.12) | 13 | 0.59 (0.03) | 0.80 (0.05) |
| <i>Pinus ponderosa</i> | -2.23 (0.14) | 21 | 0.55 (0.02) | 1.11 (0.12) |

Table 2. Turgor loss point (TLP), estimated percentage of maximum leaf hydraulic conductance ($K_{\text{leaf-max}}$) at TLP, and pre- and post-TLP capacitance (C) values from pressure–volume analyses. Numbers in parentheses are standard errors

correlated with the corresponding percentage of maximum K_{leaf} (Fig. 7a, $R^2 = 0.77$, $P < 0.01$), although the relationship was stronger with the exclusion of *Pieris* (sigmoid function fit, $R^2 = 0.91$). The percentage of full conduits at a given Ψ_L was also closely related to the percentage of cumulative acoustic emissions (Fig. 7b, $R^2 = 0.77$, $P < 0.01$).

DISCUSSION

The phenomenon of decreasing K_{leaf} with increasing water stress is well documented (e.g. Nardini *et al.* 2001; Bucci *et al.* 2003; Brodribb & Holbrook 2006; Woodruff *et al.* 2007). There are multiple potential (non-exclusive) mechanisms for dehydration-induced declines in K_{leaf} , including xylem cavitation, xylem implosion/deformation (Cochard *et al.* 2004), changes to downstream element conductivity (e.g. mesophyll) due to changes in turgor (Brodribb & Holbrook 2003) and even gene expression patterns and/or protein conformation affecting the water permeability of cell membranes (Martre *et al.* 2002; Luu & Maurel 2005).

In particular, bundle sheath cells, which are the first cells crossed by the transpiration stream as it passes from leaf

xylem to stomata, have been proposed as turgor-sensitive regulators of K_{leaf} (Sack & Holbrook 2006). Because water transport through the bundle sheath is primarily symplastic in many species (Canny 1990), the permeability of bundle sheath cell membranes can have a large impact on overall transport of water from the leaf xylem to sites of evaporation and, thus, K_{leaf} . The permeability of cell membranes can be enhanced by an order of magnitude by the expression of aquaporins (Preston *et al.* 1992), and aquaporin expression can be upregulated in response to transpirational demand (McElrone *et al.* 2007) possibly via changes in leaf turgor.

In the current study, K_{leaf} declined with increasing water stress similarly to previous studies. These decreases in K_{leaf} followed a primarily sigmoid trajectory. There has been recent debate concerning the shape of the decline in K_{leaf} with dehydration (linear versus sigmoid; Brodribb & Holbrook 2006) and the methods used to measure K_{leaf} . Although Brodribb and Holbrook observed a linear decline in K_{leaf} with dehydration, they used an evaporative flux method to measure K_{leaf} , a different method from that used in the current study. Additionally, leaf UAE curve shapes

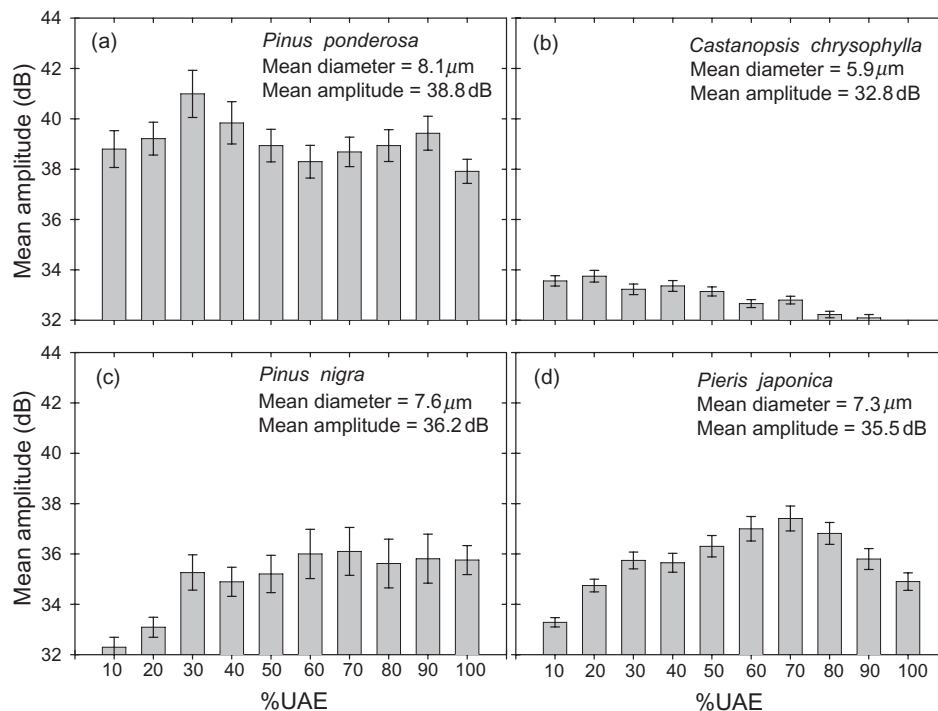


Figure 3. Mean amplitude of ultrasonic acoustic emissions (UAE) versus the percentage of total acoustic emissions in (a) *Pinus ponderosa*, (b) *Castanopsis chrysophylla*, (c) *Pinus nigra* and (d) *Pieris japonica*. Vertical error bars represent standard error.

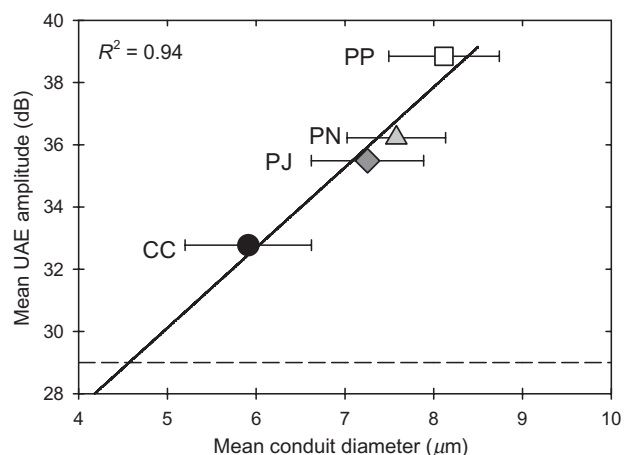


Figure 4. Mean amplitude of ultrasonic acoustic emissions (UAE) as related to mean conduit diameter. Bars represent standard errors and vertical error bars are smaller than the symbols. Dashed line represents the lower detection limit (29 dB) of the acoustic emission apparatus as used in this study. PP, *Pinus ponderosa*; PN, *Pinus nigra*; PJ, *Pieris japonica*; CC, *Castanopsis chrysophylla*.

appeared to be similar to those for eight broadleaved species measured in a previous study (Kikuta *et al.* 1997).

UAE has been used for over four decades to detect cavitation in plants (Millburn & Johnson 1966), and previous studies have shown that UAE can be used as a proxy for

measurement of hydraulic vulnerability curves in wood (e.g. Kikuta, Heitz & Richter 2003; Rosner *et al.* 2006). However, there are few available data directly comparing UAE and K_{leaf} (although there are some data for *Prunus laurocerasus* in Nardini *et al.* 2001). In the current study, there was close correspondence between K_{leaf} and UAE, indicating that the events that were impacting K_{leaf} were being detected acoustically. However, there was some offset between K_{leaf} and UAE curves in both *P. ponderosa* and *Pieris*, although the offset was in different directions. The leaf water potential corresponding to 50% loss of K_{leaf} was approximately 1 MPa more negative than the 50% UAE point in *Pieris*. It is possible that a large portion of K_{leaf} in leaves of *Pieris* is determined by properties of the extra-xylary pathway and therefore not affected by xylem embolism to the same degree as other species. Amplitudes of UAE in *Pieris* were lower at less negative water potentials and progressively increased, suggesting that smaller vessels embolized at less negative water potentials than larger ones. This could also explain the offset between K_{leaf} and UAE in *Pieris*. Additionally, many members of the Ericaceae, including *Pieris*, are known to have a layer of fibres surrounding the vascular bundle which could have some conductive function (Lems 1964). However, it is unlikely that cavitation of these fibres was detected as UAE, because they had a mean diameter of 2.8 μm , below the predicted detection threshold of the instrument.

Leaf water potentials corresponding to 50% loss of K_{leaf} in *P. ponderosa* were approximately 0.3 MPa less negative

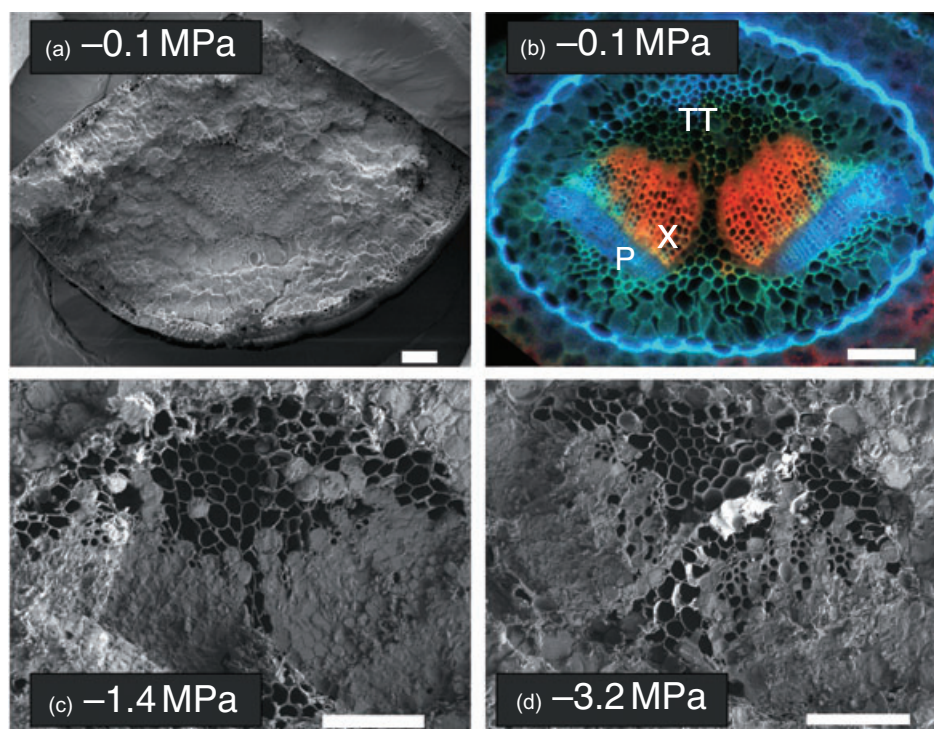


Figure 5. Cross-sections of needles of *Pinus ponderosa* (a) fully hydrated (-0.1 MPa) fluorescence image (stained with safranin dye) and (b) fully hydrated (-0.1 MPa), (c) -1.4 MPa and (d) -3.2 MPa cryo-SEM images. Scale bars represent 100 μm . X, xylem; P, pith; TT, transverse tracheids.

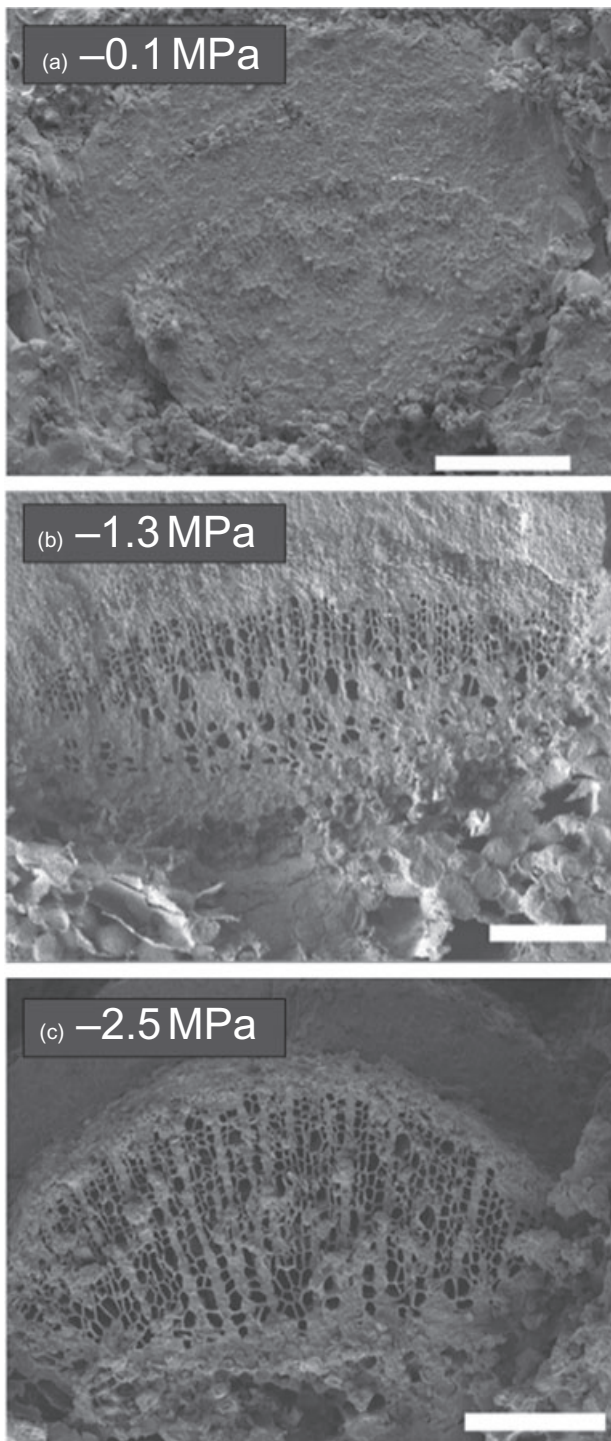


Figure 6. Cross-sections of leaf midveins of *Pieris japonica* (a) fully hydrated (-0.1 MPa), (b) -1.3 MPa and (c) -2.5 MPa cryo-SEM images. Scale bars represent $100\ \mu\text{m}$.

than the 50% UAE point. The disproportionate amount of reduction in K_{leaf} as compared to UAE may be a result of larger tracheids cavitating at less negative water potentials than smaller ones in this species, and this is supported by amplitude data (i.e. greater amplitudes over the first 20–40% of accumulated emissions, Fig. 3a).

Turgor loss points (TLPs) in the species studied here corresponded to 39–45% maximum K_{leaf} in the two broadleaved species and 13 and 21% maximum K_{leaf} in the two conifers. Brodrribb & Holbrook (2006) found that many species maintain some degree of leaf hydraulic conductance at water potentials corresponding to turgor loss. In addition, Kikuta *et al.* (1997) found that that species' leaf TLPs coincided with as little as 20% to nearly 100% cumulative UAE, and Woodruff *et al.* (2007) found TLPs that corresponded to approximately 100% loss of K_{leaf} in Douglas fir. The nature of the relationship between K_{leaf} and turgor remains unclear, but the water potential at turgor loss may be related to the minimum water potential typically experienced by leaves in their natural environment (Hao *et al.* 2008). Brodrribb & Holbrook (2006) argued that declines in K_{leaf} before (at less negative water potentials than) TLP may be related to changes in turgor in tissues downstream of the leaf xylem. However, our data do not support this hypothesis and, in fact, support the hypothesis that xylem embolism is directly related to the loss of K_{leaf} both above and below the TLP.

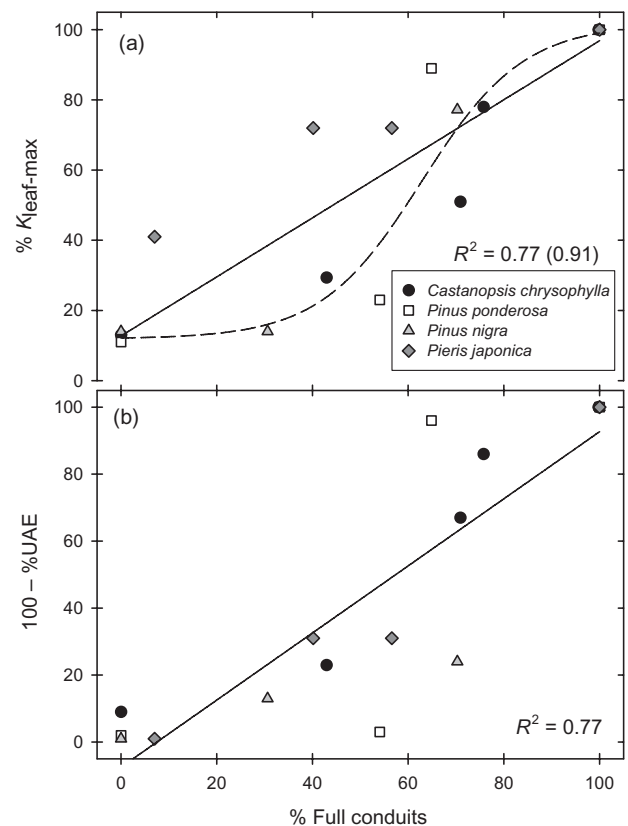


Figure 7. The relationship between (a) the percentage of full conduits and the percentage of maximum K_{leaf} . The first R^2 value and solid line refer to linear regression through all data points, while R^2 in parentheses and dashed line refer to sigmoid regression through all data except *P. japonica*. (b) Accumulated acoustic emissions as related to the percentage of full conduits.

Cryo-SEM images confirmed that cavitation occurred proportionally to the loss of K_{leaf} and accumulated UAE in these species. In addition, there was a close relationship between mean conduit diameter and UAE amplitude, and the lower conduit diameter limit for detection of cavitation events by UAE was approximately 4.5 μm . Therefore, cavitation in species with smaller leaf xylem conduits or some of the smaller conduits in species used in the current study may not be detectable with this method. The majority of transfusion tissue surrounding the vascular bundles in *P. ponderosa* was empty at a leaf water potential corresponding to 4% of accumulated UAE and approximately 92% of maximum K_{leaf} . This transfusion tissue appears to be made up of dead cells that are lignified and pitted and may therefore be a type of tracheid (see also Gambles & Dengler 1982; Canny 1993; Meicenheimer, Coffin & Chapman 2008). However, until more detailed anatomical studies can be performed, we will refer to this tissue simply as transfusion tissue.

It is likely that the transfusion tissue surrounding the vascular bundles in this species empties via a different mechanism than xylem tracheids (no UAE detected for the emptying of transfusion tissue), and although the cells that make up this tissue are much larger in diameter, they contribute a small fraction to K_{leaf} as compared to xylem tracheids. This is in contrast to an earlier study that reported declines in K_{leaf} that were correlated with the collapse of accessory transfusion tracheids in a *P. grayi* (Brodrribb & Holbrook 2005), although these accessory tracheids were oriented differently (extended from near the vascular tissue into the mesophyll, whereas *P. ponderosa* transfusion tissue was confined within the endodermis) and, presumably, functionally different from transfusion tracheids in *P. grayi*. Another earlier study suggested that dehydration-induced reductions in K_{leaf} of several *Pinus* species were due to xylem tracheid deformation (Cochard *et al.* 2004). However, it should be noted that we saw no evidence of deformation or collapse in either *P. nigra* or *P. ponderosa* xylem tracheids (or vessels of the two angiosperm species). One possible role for this transfusion tissue in *P. ponderosa* could be as a large source of capacitance. If this tissue is primarily for water storage, then it is likely that conifers, which typically have this tissue type (Gadek & Quinn 1988), may have generally higher leaf capacitance than angiosperm tree species, which appear to lack this tissue. In fact, in an earlier study, conifer species of southern Chile were found to have much greater leaf capacitance than co-occurring angiosperms (Brodrribb *et al.* 2005).

More work is needed on other species to determine the extent to which the reported trends in K_{leaf} , UAE and xylem embolism are universal. It will also be important to address the contributions of different tissues (and also contributions due to gene expression patterns/membrane protein conformational changes) to K_{leaf} , especially during leaf dehydration. Finally, *in situ* K_{leaf} measurements in the field, along with measurements of leaf gas exchange and water status, may help us to better understand the relationships between K_{leaf} , stomatal behaviour and photosynthesis.

ACKNOWLEDGMENTS

This research was supported in part by National Science Foundation grant IOB-0544470. The authors would like to thank Logan Barnart and Matthew Wibbenmeyer for their helpful assistance in the lab and Peter Kitin and Derrick Horne for microscopy and imaging. We are also grateful to Dr Barbara Lachenbruch for critical discussion of ideas.

REFERENCES

- Abramoff M.D., Magelhaes P.J. & Ram S.J. (2004) Image processing with image. *J Biophotonics International* **11**, 36–42.
- Brodrribb T.J. & Holbrook N.M. (2003) Stomatal closure during leaf dehydration, correlation with other leaf physiological traits. *Plant Physiology* **132**, 2166–2173.
- Brodrribb T.J. & Holbrook N.M. (2005) Water stress deforms tracheids peripheral to the leaf vein of a tropical conifer. *Plant Physiology* **137**, 1139–1146.
- Brodrribb T.J. & Holbrook N.M. (2006) Declining hydraulic efficiency as transpiring leaves desiccate: two types of response. *Plant, Cell & Environment* **29**, 2205–2215.
- Brodrribb T.J., Holbrook N.M., Zwieniecki M.A. & Palma B. (2005) Leaf hydraulic capacity in ferns, conifers and angiosperms: impacts on photosynthetic maxima. *New Phytologist* **165**, 839–846.
- Brodrribb T.J., Field T.S. & Jordan G.J. (2007) Leaf maximum photosynthetic rate and venation are linked by hydraulics. *Plant Physiology* **144**, 1890–1898.
- Bucci S.J., Scholz F.G., Goldstein G., Meinzer F.C., Sternberg L., Da S.L. (2003) Dynamic changes in hydraulic conductivity in petioles of two savanna tree species: factors and mechanisms contributing to the refilling of embolized vessels. *Plant, Cell & Environment* **26**, 1633–1645.
- Canny M.J. (1990) What becomes of the transpiration stream? *New Phytologist* **114**, 341–368.
- Canny M.J. (1993) Transfusion tissue of pine needles as a site of retrieval of solutes from the transpiration stream. *New Phytologist* **123**, 227–232.
- Cochard H., Froux F., Mayr S. & Coutand C. (2004) Xylem wall collapse in water-stressed pine needles. *Plant Physiology* **134**, 401–408.
- Cochard H., Venisse J.-S., Barigah T.S., Brunel N., Harbette S., Guilliot A., Tyree M.T. & Sakr S. (2007) Putative role of aquaporins in variable hydraulic conductance of leaves in response to light. *Plant Physiology* **143**, 122–133.
- Gadek P.A. & Quinn C.J. (1988) Pitting of transfusion tracheids in Cupressaceae. *Australian Journal of Botany* **36**, 81–92.
- Gambles R.L. & Dengler R.E. (1982) The anatomy of the leaf of red pine, *Pinus resinosa*. II. Vascular tissues. *Canadian Journal of Botany* **60**, 2804–2824.
- Hacke U.G., Sperry J.S., Pockman W.T., Davis S.D. & McCulloh K. (2001) Trends in wood density and structure are linked to prevention of xylem implosion by negative pressure. *Oecologia* **126**, 457–461.
- Hacke U.G., Sperry J.S. & Pittermann J. (2004) Analysis of circular bordered pit function II. Gymnosperm tracheids with torus-margo pit membranes. *American Journal of Botany* **91**, 386–400.
- Hao G., Hoffmann W.A., Scholz F.G., Bucci S.J., Meinzer F.C., Franco A.C., Cao K. & Goldstein G. (2008) Stem and leaf hydraulics of congeneric tree species from adjacent tropical savanna and forest ecosystems. *Oecologia* **155**, 405–415.
- Kaldenhoff R., Ribas-Carbo M., Flexas Sans J., Lovisolo C., Heckwolf M. & Uehlein N. (2008) Aquaporins and plant water balance. *Plant, Cell & Environment* **31**, 658–666.

- Kikuta S.B., Lo Gullo M.A., Nardini A., Richter H. & Salleo S. (1997) Ultrasound acoustic emissions from dehydrating leaves of deciduous and evergreen trees. *Plant, Cell & Environment* **20**, 1381–1390.
- Kikuta S.B., Heitz P. & Richter H. (2003) Vulnerability curves from conifer sapwood sections exposed over solutions with known water potentials. *Journal of Experimental Botany* **54**, 2149–2155.
- Lems K. (1964) Evolutionary studies in the Ericaceae. II. Leaf anatomy is a phylogenetic index in the Andromedeae. *Botanical Gazette* **125**, 178–186.
- Luu D.T. & Maurel C. (2005) Aquaporins in a challenging environment: molecular gears for adjusting plant water status. *Plant, Cell & Environment* **28**, 85–96.
- McElrone A.J., Bichler J., Pockmann W.T., Addington R.N., Linder C.R. & Jackson R.B. (2007) Aquaporin-mediated changes in hydraulic conductivity of deep tree roots accessed via caves. *Plant, Cell & Environment* **30**, 1411–1421.
- Martre P., Morillon R., Barrieu F., North G.B., Nobel P.S. & Chrispeels M.J. (2002) Plasma membrane aquaporins play a significant role during recovery from water deficit. *Plant Physiology* **130**, 2101–2110.
- Meicenheimer R.D., Coffin D.W. & Chapman E.M. (2008) Anatomical basis for biophysical differences between *Pinus nigra* and *P. resinosa* (Pinaceae) leaves. *American Journal of Botany* **95**, 1191–1198.
- Millburn J.A. & Johnson R.P.C. (1966) The conduction of sap. I. Detection of vibrations produced by sap cavitation in *Ricinus* xylem. *Planta* **69**, 43–52.
- Mott K.A. (2007) Leaf hydraulic conductivity and stomatal responses to humidity in amphistomatous leaves. *Plant, Cell & Environment* **30**, 1444–1449.
- Nardini A. & Salleo S. (2000) Limitation of stomatal conductance by hydraulic traits: sensing or preventing xylem cavitation? *Trees* **15**, 14–24.
- Nardini A. & Salleo S. (2005) Water stress-induced modification in leaf hydraulic architecture in sunflower: co-ordination with gas exchange. *Journal of Experimental Botany* **56**, 3093–3101.
- Nardini A., Tyree M.T. & Salleo S. (2001) Xylem cavitation in the leaf of *Prunus laurocerasus* and its impact on leaf hydraulics. *Plant Physiology* **125**, 1700–1709.
- Nardini A., Salleo S. & Raimondo F. (2003) Changes in leaf hydraulic conductance correlate with leaf vein embolism in *Cercis siliquastrum* L. *Trees* **17**, 529–534.
- Preston G.M., Carroll T.P., Guggino W.B. & Agree P. (1992) Appearance of water channels in *Xenopus oocytes* expressing red cell CHIP 28 proteins. *Science* **256**, 385–387.
- Ritman K.T. & Milburn J.A. (1988) Acoustic emissions from plants: ultrasonic and audible compared. *Journal of Experimental Botany* **38**, 1237–1248.
- Ritman K.T. & Milburn J.A. (1991) Monitoring of ultrasonic and audible emissions from plants with or without vessels. *Journal of Experimental Botany* **42**, 123–130.
- Rosner S., Klien A., Wimmer R. & Karlsson B. (2006) Extraction of features from ultrasonic acoustic emissions: a tool to assess the hydraulic vulnerability of Norway spruce trunkwood? *New Phytologist* **171**, 105–116.
- Sack L. & Holbrook N.M. (2006) Leaf hydraulics. *Annual Review of Plant Biology* **57**, 361–381.
- Sack L., Streeter C.M. & Holbrook N.M. (2004) Hydraulic analysis of water flow through leaves of sugar maple and red oak. *Plant Physiology* **134**, 1824–1833.
- Salleo S., Nardini A., Pitt F. & Lo Gullo M.A. (2001) Xylem cavitation and hydraulic control of stomatal conductance in Laurel (*Laurus nobilis* L.). *Plant, Cell & Environment* **23**, 71–79.
- Scholander P.F., Hammel H.T., Bradstreet E.D. & Hemmington E.A. (1965) Sap pressure in vascular plants. *Science* **148**, 339–346.
- Tyree M.T. & Dixon M.A. (1983) Cavitation events in *Thuja occidentalis*. Ultrasonic acoustic emissions from the sapwood can be measured. *Plant Physiology* **72**, 1094–1099.
- Tyree M.T. & Hammel H.T. (1972) The measurement of the turgor pressure and the water relations of plants by the pressure-bomb technique. *Journal of Experimental Botany* **23**, 267–282.
- Tyree M.T. & Sperry J.S. (1989) Vulnerability of xylem to cavitation and embolism. *Annual Review of Plant Physiology and Molecular Biology* **40**, 19–38.
- Tyree M.T. & Yang S. (1992) Hydraulic conductivity recovery versus water pressure in xylem of *Acer saccharum*. *Plant Physiology* **100**, 669–676.
- Voicu M.C., Zwiazek J.J. & Tyree M.T. (2008) Light response of hydraulic conductance in bur oak (*Quercus macrocarpa*) leaves. *Tree Physiology* **28**, 1007–1015.
- Woodruff D.R., McCulloh K.A., Warren J.R., Meinzer F.C. & Lachenbruch B. (2007) Impacts of tree height on leaf hydraulic architecture and stomatal control in Douglas-fir. *Plant, Cell & Environment* **30**, 559–569.

Received 8 December 2008; accepted for publication 26 January 2009